IL NUOVO CIMENTO **41 C** (2018) 150
DOI 10.1393/ncc/i2018-18150-4

Colloquia: LaThuile 2018

Measurements and combination of $\sin^2\theta_{\mathrm{eff}}^{\mathrm{lept}}$ at the Tevatron

B. Quinn(*)(**)
University of Mississippi - Oxford, MS, USA

received 6 September 2018

Summary. — We present the combination of measurements of the effective-leptonic weak mixing angle parameter $\sin^2\theta_{\mathrm{eff}}^{\mathrm{lept}}$ from the CDF and D0 experiments using the full Tevatron data sets. The standard model weak mixing angle parameter $\sin^2\theta_W$ and equivalent value of M_W are inferred based on ZFITTER calculations. These Tevatron measurements are consistent with the world-best measurements from electron-positron colliders. The uncertainties represent the best precision from hadron colliders, nearly matching that of the best electron-positron individual measurements.

1. – Introduction

Drell-Yan lepton pairs [1] are produced at Fermilab's Tevatron through the reaction $q\bar{q} \rightarrow \gamma^*/Z \rightarrow \ell^+\ell^-$ in $p\bar{p}$ collisions at $\sqrt{s} = 1.96$ TeV. At the Born level, fermions interact through vector coupling to the virtual photon ($g_V^f = Q_f$), and through vector and axial vector coupling to the Z boson ($g_V^f = I_3 - 2Q_f \sin^2\theta_W$, $g_A^f = I_3$). In the Born-level standard model (SM), and to all orders of the on-shell renormalization scheme [2], $\sin^2\theta_W = 1 - M_W^2/M_Z^2$, and since M_z is known to high precision (± 0.0021 GeV/c^2 [3,4]), a $\sin^2\theta_W$ inference is equivalent to an indirect M_W measurement. Weak-interaction radiative corrections of a few percent alter the Born-level couplings to give the effective weak-mixing parameter, $\sin^2\theta_{\mathrm{eff}}^{\mathrm{lept}}$. The forward-backward asymmetry of the polar-angle distribution of the Drell-Yan $\ell^+\ell^-$ pairs is sensitive to $\sin^2\theta_{\mathrm{eff}}^{\mathrm{lept}}$, and thus indirectly to $\sin^2\theta_W$ in the context of the SM. The average of six individual measurements from the LEP-1 and SLC lepton colliders is 0.23149 ± 0.00016. However, there is a 3.2 standard-deviation difference between the two most precise individual measurements [3,4]. This provides strong motivation for an accurate complementary determination of $\sin^2\theta_{\mathrm{eff}}^{\mathrm{lept}}$ by the Tevatron hadron collider experiments.

(*) E-mail: quinn@phy.olemiss.edu
(**) On behalf of the CDF and D0 Collaborations.

The $\ell^+\ell^-$ angular distribution is measured in the Collins-Soper rest frame of the boson, in which the polar angle ϑ of the ℓ^- is defined relative to the incoming quark direction [5]. Forward (backward) events are designated as those with $\cos\vartheta \geq 0$ ($\cos\vartheta < 0$). The general expression for the angular distribution includes nine helicity cross section terms that reduce to $\mathrm{d}N/\mathrm{d}\Omega \propto 1 + \cos^2\vartheta + A_4\cos\vartheta$ [6, 7] at zero transverse momentum, where the distribution is azimuthally symmetric. The A_4 term which arises from the interference of vector and axial-vector amplitudes is parity violating and induces a forward-backward asymmetry in $\cos\vartheta$. The $\gamma^* - Z$ interference is independent of $\sin^2\theta_W$, zero at the Z pole, and dominant away from the Z pole. Sensitivity to the weak mixing angle comes through the Z self-interference, which dominates near the Z-pole mass. The forward-backward asymmetry as a function of the dilepton mass, M, is defined as

$$A_{\mathrm{fb}}(M) = \frac{\sigma^+(M) - \sigma^-(M)}{\sigma^+(M) + \sigma^-(M)} = \frac{3}{8}A_4(M), \tag{1}$$

where $\sigma^{+(-)}$ is the forward (backward) cross section.

The CDF [8] and D0 [9-11] experiments employ general-purpose detectors for hadron collision measurements. They each include central charged-particle trackers in solenoid fields, electromagnetic and hadronic calorimeters, and outer hadron absorbers and trackers for muon identification. Both CDF and D0 measure A_{fb} with high-p_{T} electron and muon pairs. The measurement strategy for each of the four separate analyses consists of four steps: measure A_{fb} in bins of M, generate simulation templates of $A_{\mathrm{fb}}(M, \sin^2\theta_W)$ at several values of the weak-mixing angle, perform full corrections (*e.g.* for detector and higher-order QCD effects) to data and simulation events, and extract $\sin^2\theta^{\mathrm{lept}}_{\mathrm{eff}}$ using a χ^2 comparison between the data and templates to determine the prediction that best fits the measured $A_{\mathrm{fb}}(M)$ distribution.

2. – CDF measurements

The CDF electron [12] and muon [13] channel measurements utilize the full Tevatron Run II data set consisting of 9 fb^{-1} of integrated luminosity. Kinematic, fiducial, lepton-identification, and isolation selection criteria are applied to yield final samples of approximately 485000 electron pairs and 277000 muon pairs.

A powerful feature of the A_{fb} measurements is a data-driven event-weighting method [14], which essentially combines individual measurements in $|\cos\vartheta|$ bins. The asymmetry for an individual bin is

$$A_{\mathrm{fb}} = \frac{N^+/(\epsilon A)^+ - N^-/(\epsilon A)^-}{N^+/(\epsilon A)^+ + N^-/(\epsilon A)^-}, \tag{2}$$

where $N^{+(-)}$ and $(\epsilon A)^{+(-)}$ are the event count, and the efficiency and acceptance product, respectively, of forward (backward) lepton pairs. The CDF detector is roughly charge symmetric, so interchanging the lepton charges will reverse the sign of $\cos\vartheta$ but will not change which detector cells are traversed by the pair or the lepton momentum in a cell. Therefore, the (ϵA) dependence cancels to first order so

$$A_{\mathrm{fb}} \approx \frac{N^+ - N^-}{N^+ + N^-}. \tag{3}$$

The event weights in the numerator and denominator remove angular dependencies of the event difference and sum, and provide the appropriate statistical weight for combining events across $|\cos\vartheta|$ bins. The event-weighting method requires sufficiently high statistics for each bin, so the pseudorapidity acceptance is restricted. In the electron channel, one electron must be central ($0.05 < |\eta_{\rm det}| < 1.05$) while the other can be either in the central or forward ($1.2 < |\eta_{\rm det}| < 2.8$) region; in the muon channel, both muons must be in the central region ($|\eta_{\rm det}| < 1$).

The simulation of Drell-Yan events uses PYTHIA 6.2 [15] with CTEQ5L [16] PDFs and PHOTOS 2.0 [17] to generate events including QED FSR. The detector simulation that follows is based on GEANT-3 and GFLASH [18]. Corrections due to higher order QCD effects are applied to generated events to adjust distributions for better agreement between data and simulation. Energy scales for data and simulation are calibrated to a common standard [19]. Additional tuning is performed to enable matrix unfolding of $A_{\rm fb}$ in mass and $\cos\vartheta$, which removes the effects of resolution smearing and QED FSR. QCD dijet backgrounds are determined from data, while backgrounds from $W+$ jets, $\gamma^*/Z \to \tau\tau$, diboson (WW, WZ, and ZZ), and $t\bar{t}$ events are estimated with PYTHIA 6.2. The overall background level is 1.1% for the electron channel and 0.5% for the muon channel. The $A_{\rm fb}$ templates are calculated using next-to-leading-order (NLO) POWHEG-BOX [20, 21] with PYTHIA 6.41 [22] and NNPDF 3.0 [23] next-to-next-to-leading order (NNLO) PDFs. Complex-valued form factor corrections to the effective couplings are calculated with ZFITTER 6.43 [24], providing an enhanced Born approximation (EBA) to the electroweak couplings.

The value of $\sin^2\theta^{\rm lept}_{\rm eff}$ extracted from the asymmetry measurement in the electron channel [12] is $\sin^2\theta^{\rm lept}_{\rm eff} = 0.23248 \pm 0.00049({\rm stat}) \pm 0.00004({\rm syst}) \pm 0.00019({\rm PDF})$. The result is $\sin^2\theta^{\rm lept}_{\rm eff} = 0.2315 \pm 0.0009({\rm stat}) \pm 0.0002({\rm syst}) \pm 0.0004$ (PDF) for the muon-channel [13]. The PDF uncertainties dominate the other systematic uncertainties which include contributions from the energy scale and resolution, the backgrounds, and the QCD scale. The CDF result obtained by combining electron and muon channels [12] is

$$\sin^2\theta^{\rm lept}_{\rm eff} = 0.23221 \pm\ 0.00043({\rm stat}) \pm\ 0.00007({\rm syst}) \pm\ 0.00016({\rm PDF}), \tag{4}$$

where the PDF uncertainty has been reduced through the use of the GK weighting method which incorporates PDF information from the asymmetry measurements in both channels [25, 26].

3. – D0 measurements

The D0 measurements of $\sin^2\theta^{\rm lept}_{\rm eff}$ in the electron [27] and muon [28] channels use 9.7 fb^{-1} and 8.6 fb^{-1} of recorded luminosity, respectively. Very high statistics samples are selected by accepting leptons over wide $\eta_{\rm det}$ ranges for electrons ($|\eta_{\rm det}| < 1.1$ in the central calorimeter (CC) and $1.5 < |\eta_{\rm det}| < 3.2$ in the end calorimeter (EC)) and muons ($|\eta_{\rm det}| < 1.8$). This results in final samples of approximately 560000 electron pairs and 481000 muon pairs.

The Drell-Yan signal events are simulated using PYTHIA 6.23 [15] with NNPDF 2.3 [29] PDFs for the electron channel and NNPDF 3.0 PDFs for the muon channel, followed by a GEANT-based detector simulation [30]. The solenoid and toroid magnet polarities are reversed every two weeks at D0, so separate simulation samples for the four different polarity combinations are generated and used to model the corresponding data samples. The samples are then weighted to correspond to equal luminosity exposures for each polarity combination, thus providing cancellation of asymmetries due to detector response variations. New methods of electron energy and muon momentum calibration are applied to data and simulation. These calibrations include scale and offset parameters applied to electron energy as functions of $\eta_{\rm det}$ and instantaneous luminosity, and a muon momentum scale factor dependent on charge, $\eta_{\rm det}$, and solenoid polarity. With these methods, energy and momentum modeling systematic uncertainties are reduced to negligible levels. Backgrounds from multijet events are determined from the data and $W+$jets, $\gamma^*/Z \to \tau\tau$, diboson, and $t\bar{t}$ events are estimated with ALPGEN [31] and PYTHIA 6.23, finding that overall background levels in the electron and muon channels are 0.35% and 0.88%, respectively. The D0 $A_{\rm fb}$ templates are calculated using PYTHIA 6.23 with NNPDF 2.3 (electron channel) and NNPDF 3.0 (muon channel). The templates are reweighted to incorporate higher-order QCD effects, and processed by the D0 detector simulation to include detector resolution effects. For the electron channel, $A_{\rm fb}$ distributions are measured separately for CC-CC, CC-EC, and EC-EC event categories.

The three electron event category measurements are combined to obtain the electron-channel result $\sin^2\theta^{\rm lept}_{\rm eff} = 0.23139 \pm 0.00043({\rm stat}) \pm 0.00008({\rm syst}) \pm 0.00017({\rm PDF})$. Again, the PDF uncertainty dominates the other sources of systematic uncertainty which include energy calibration and smearing, backgrounds, and charge and electron misidentification [27]. The muon channel extraction gives $\sin^2\theta^{\rm lept}_{\rm eff} = 0.22994 \pm 0.00059({\rm stat}) \pm 0.00005({\rm syst}) \pm 0.00024({\rm PDF})$. Non-PDF systematic uncertainties stem from momentum calibration and smearing, backgrounds, and muon misidentification [28].

The CDF and D0 analyses use different methods for weak-interaction radiative corrections, and the D0 electron-channel measurement differs from the other three in its use of NNPDF 2.3. Corrections are applied to the D0 $\sin^2\theta^{\rm lept}_{\rm eff}$ values above to standardize all Tevatron results to a "common framework" using the ZFITTER EBA radiative correction implementation and NNPDF3.0. The D0 $A_{\rm fb}$ templates are calculated with PYTHIA, which uses the same fixed value of $\sin^2\theta^{\rm lept}_{\rm eff}$ for all fermions. The ZFITTER weak-interaction corrections used for the CDF templates include fermion-dependent form factors and the fermion-loop correction to the photon propagator, which are complex valued and mass-scale dependent. The difference between the two approaches is found to be $\Delta\sin^2\theta^{\rm lept}_{\rm eff}(\textsc{zfitter}) = +0.00022 \pm 0.00004$. A D0 comparison of NNPDF 2.3 and NNPDF 3.0 ensembles finds a difference in extracted $\sin^2\theta^{\rm lept}_{\rm eff}$ values which requires a correction of $\Delta\sin^2\theta^{\rm lept}_{\rm eff}({\rm PDF}) = -0.00024 \pm 0.00004$, to standardize the D0 NNPDF 2.3 electron measurement to one made with NNPDF 3.0. After applying $\Delta\sin^2\theta^{\rm lept}_{\rm eff}({\rm PDF})$ to the electron-channel result and $\Delta\sin^2\theta^{\rm lept}_{\rm eff}(\textsc{zfitter})$ to both channels, the corrected values are $\sin^2\theta^{\rm lept}_{\rm eff} = 0.23137 \pm 0.00043({\rm stat}) \pm 0.00009({\rm syst}) \pm 0.00017({\rm PDF})$ for electrons and $\sin^2\theta^{\rm lept}_{\rm eff} = 0.23016 \pm 0.00059({\rm stat}) \pm 0.00006({\rm syst}) \pm 0.00024({\rm PDF})$ for muons. Combining these corrected D0 electron- and muon-channel results gives

$$\sin^2\theta^{\rm lept}_{\rm eff} = 0.23095 \pm\ 0.00035({\rm stat}) \pm\ 0.00007({\rm syst}) \pm\ 0.00019({\rm PDF}). \tag{5}$$

4. – CDF and D0 combination

The electron- and muon-channel combination results from CDF and D0 are combined using the "best linear unbiased estimate" (BLUE) method [32]. The PDF uncertainties on the inputs are considered to be 100% correlated and all other systematic uncertainties are treated as uncorrelated. This yields a Tevatron combination value of

$$\sin^2\theta^{\rm lept}_{\rm eff} = 0.23148 \pm\ 0.00027({\rm stat}) \pm\ 0.00005({\rm syst}) \pm\ 0.00018({\rm PDF}). \tag{6}$$

The combination weights are 0.42 for the CDF input and 0.58 for the D0 input, with a combination χ^2 probability of 2.6%. The inference of $\sin^2\theta_W$ (and equivaently, M_W) from the direct measurement of $\sin^2\theta^{\rm lept}_{\rm eff}$ is made through the relationship $\sin^2\theta^{\rm lept}_{\rm eff} = {\rm Re}[\kappa_e(\sin^2\theta_W, M_Z^2)]\sin^2\theta_W$ and with a ZFITTER calculation of the form factor ${\rm Re}[\kappa_e] = 1.0371$. This gives Tevatron combination values of $\sin^2\theta_W = 0.22324 \pm 0.00026({\rm stat}) \pm 0.00019({\rm syst})$ and $M_W = 80.367 \pm 0.014({\rm stat}) \pm 0.010({\rm syst})\ {\rm GeV}/c^2$. The Tevatron measurements of $\sin^2\theta^{\rm lept}_{\rm eff}$ presented here are compared with previous results from the Z-pole region in fig. 1 [3, 33-35]. The W-boson mass inference is compared in fig. 2 with previous direct [36] and indirect [3, 4] measurements.

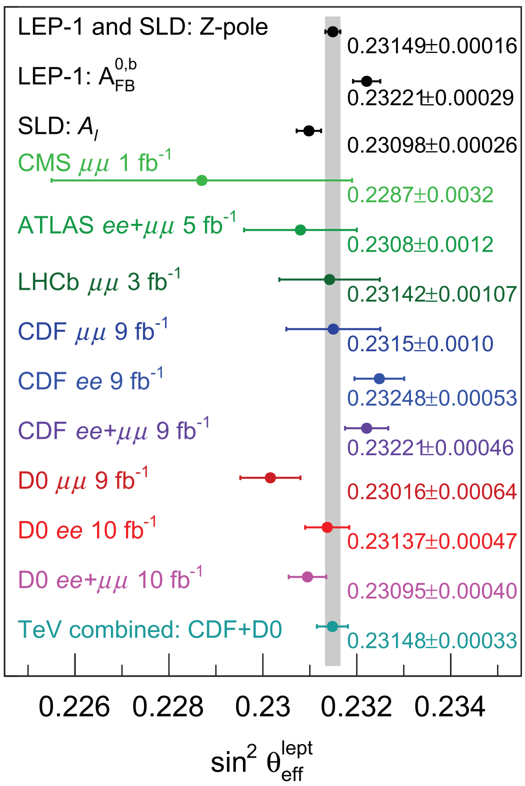

Fig. 1. – Comparison of experimental measurements of $\sin^2\theta^{\rm lept}_{\rm eff}$ in the region of the Z-boson pole mass. The horizontal bars represent total uncertainties. The LEP-1 and SLD Z pole result is the combination of their six measurements, and the shaded vertical band shows its uncertainty.

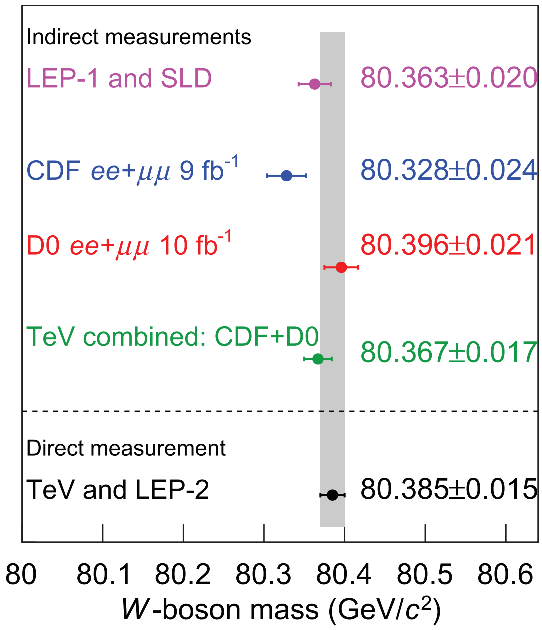

Fig. 2. – Comparison of experimental determinations of the W-boson mass. The horizontal bars represent total uncertainties. The shaded vertical band shows the uncertainty of the direct measurements.

5. – Conclusions

The effective-leptonic weak mixing parameter $\sin^2\theta^{\rm lept}_{\rm eff}$ is determined from measurements of Drell-Yan forward-backward asymmetry by the CDF and D0 experiments in both the electron and muon channels using the full Tevatron RunII data set. Inferences of $\sin^2\theta_W$ and M_W based on standard model calculations are also made. The Tevatron combination results are

$$\sin^2\theta^{\rm lept}_{\rm eff} = 0.23148 \pm 0.00033, \tag{7a}$$

$$\sin^2\theta_W = 0.22324 \pm 0.00033, \text{ and} \tag{7b}$$

$$M_W = 80.367 \pm 0.017 \text{ GeV}/c^2. \tag{7c}$$

These represent the best precision from hadron colliders, approaching the best individual measurements from LEP-1 and SLD. Although it does not resolve the long-standing 3.2σ difference between the lepton collider results, the Tevatron value for $\sin^2\theta^{\rm lept}_{\rm eff}$ perhaps removes some of the tension due to the fact that it falls squarely on the world average, and is consistent with both. The $17\,\text{MeV}/c^2$ uncertainty on the Tevatron inference of M_W comes very close to the uncertainty on the combination of direct measurements from the Tevatron and LEP-2, providing a powerful test of SM self-consistency.

* * *

The author would like to thank the staffs at Fermilab and collaborating institutions, and acknowledge support from the U.S. Department of Energy.

REFERENCES

[1] Drell S. D. and Yan T.-M., *Phys. Rev. Lett.*, **25** (1970) 316.
[2] Sirlin A., *Phys. Rev. D*, **22** (1980) 971.
[3] The ALEPH, DELPHI, L3, OPAL, SLD Collaborations, the LEP Electroweak Working Group, the SLD Electroweak and Heavy Flavour Groups, *Phys. Rep.*, **427** (2006) 257.
[4] The ALEPH, DELPHI, L3, OPAL Collaborations, the LEP Electroweak Working Group, *Phys. Rep.*, **532** (2013) 119.
[5] Collins J. C. and Soper D. E., *Phys. Rev. D*, **16** (1977) 2219.
[6] Mirkes E., *Nucl. Phys. B*, **387** (1992) 3.
[7] Mirkes E. and Ohnemus J., *Phys. Rev. D*, **50** (1994) 5692.
[8] Abulencia A. *et al.*, *J. Phys. G*, **34** (2007) 2457.
[9] Abazov V. M. *et al.*, *Nucl. Instrum. Methods Phys. Res. Sect. A*, **565** (2006) 463.
[10] Abolins M. *et al.*, *Nucl. Instrum. Methods Phys. Res. Sect. A*, **584** (2008) 75.
[11] Angstadt R. *et al.*, *Nucl. Instrum. Methods Phys. Res. Sect. A*, **622** (2010) 298.
[12] Aaltonen T. *et al.*, *Phys. Rev. D*, **93** (2016) 112016.
[13] Aaltonen T. *et al.*, *Phys. Rev. D*, **89** (2014) 072005.
[14] Bodek A., *Eur. Phys. J. C*, **67** (2010) 321.
[15] Sjöstrand T., Edén P., Lönnblad L., Miu G., Mrenna S. and Norrbin E., *Comput. Phys. Commun.*, **135** (2001) 238.
[16] Lai H. L. *et al.*, *Eur. Phys. J. C*, **12** (2000) 375.
[17] Barberio E. and Was Z., *Comput. Phys. Comm.*, **79** (1994) 291.
[18] Grindhammer G., Rudowicz M. and Peters S., *Nucl. Instrum. Methods Phys. Res. Sect. A*, **290** (1990) 469.
[19] Bodek A., van Dyne A., Han J.-Y., Sakumoto W. and Strelnikov A., *Eur. Phys. J. C*, **72** (2012) 2194.
[20] Frixione S., Nason P. and Oleari C., *JHEP*, **11** (2007) 070.
[21] Alioli S., Nason P., Oleari C. and Re E., *JHEP*, **07** (2008) 060.
[22] Sjöstrand T., Mrenna S. and Skands P. Z., *JHEP*, **05** (2006) 026.
[23] Ball R. D. *et al.*, *JHEP*, **04** (2015) 040.
[24] Arbuzov A., Awramik M., Czakon M., Freitas A., Grünewald M., Monig K., Riemann S. and Riemann T., *Comput. Phys. Commun.*, **174** (2006) 728.
[25] Giele W. T. and Keller S., *Phys. Rev. D*, **58** (1998) 094023.
[26] Bodek A., Han J.-Y., Khukhunaishvili A. and Sakumoto W., *Eur. Phys. J. C*, **76** (2016) 115.
[27] Abazov V. M. *et al.*, *Phys. Rev. Lett.*, **115** (2015) 041801.
[28] Abazov V. M. *et al.*, *Phys. Rev. Lett*, **120** (2018) 241802, arXiv:1710.03951 [hep-ex].
[29] Ball R. D. *et al.*, *Nucl. Phys. B*, **867** (2013) 244.
[30] Brun R. and Carminati F. (1993) unpublished.
[31] Mangano M. L. *et al.*, *JHEP*, **07** (2003) 001.
[32] Lyons L., Gibaut D. and Cliffort P., *Nucl. Instrum. Methods Phys. Res. Sect. A*, **270** (1988) 110.
[33] Chatrchyan S. *et al.*, *Phys. Rev. D*, **84** (2011) 112002.
[34] Aad G. *et al.*, *JHEP*, **09** (2015) 049.
[35] Aaij R. *et al.*, *JHEP*, **11** (2015) 190.
[36] Aaltonen T. *et al.*, *Phys. Rev. D*, **88** (2013) 052018.